Journal of the Chinese Institute of Engineers, Vol. 23, No. 3, pp. 349-356 (2000)

ADAPTIVE INTEGRATION IN ELASTO-PLASTIC BOUNDARY ELEMENT ANALYSIS

Xiao-Wei Gao and Trevor G. Davies
Department of Civil Engineering
Glasgow University
Glasgow G12 8LT, UK

Key Words: addaptive integration, elasto-plasticity, boundary element method.

ABSTRACT

This paper describes an efficient adaptive integration technique for both internal cell integration and boundary element integration. The adaptive algorithm can cope with the common situation where the sizes of adjacent cells and boundary elements are significantly different. Various cases are examined numerically and some numerical applications demonstrate the effectiveness of this method.

I. INTRODUCTION

In non-linear boundary element analyses, accurate and efficient integration of the initial stress (or strain) kernels over internal cells is crucial. While the singular domain integrals can be accurately evaluated using special techniques, the nearly singular integrals which arise when source and field points are in close proximity can require many (expensive) functional evaluations. The usual way to deal with volume integrals (over cells) is to divide the cells into sufficient sub-cells and employ multi-dimensional Gauss quadrature. This method was first coded by Mustoe (1984) using a criterion described by Lachat and Watson (1976) for the upper bound of relative error. Mustoe's method does not introduce extra nodes and is equivalent to densifying the Gauss points towards the singularity.

In this paper, efficient adaptive integration techniques for elastoplastic BEM are developed, based on two criteria. The first is an extension of Lachat and Watson's (1976) method and a practical implementation of this method is described. The second is a development of Davies and Bu's (1995) method for the integration of boundary integrals. If the required Gauss integration order exceeds a specified maximum, cells are divided into sub-cells. This technique can deal with both internal cell integrations and boundary element integrations. Further, the adaptive algorithm can cope with the common situation where the sizes of adjacent cells are significantly different. Some illustrative cases are examined numerically, in both two and three dimensions.

II. SINGULARITIES IN ELASTOPLASTIC BEM EQUATIONS

The direct elastoplastic BEM equations, using the initial stress approach, can be written as (Telles, 1983; Banerjee and Davies, 1984)

$$c_{ij}\dot{u}_j + \int_\Gamma T_{ij}\dot{u}_j d\Gamma = \int_\Gamma U_{ij}\dot{t}_j d\Gamma + \int_\Omega E_{ijk}\dot{\sigma}^p_{jk} d\Omega \qquad (1)$$

where $c_{ij}=1/2\delta_{ij}$ for smooth boundary points and $c_{ij}=\delta_{ij}$ for interior points; U_{ij} and T_{ij} are the Kelvin's fundamental solutions for displacements and tractions and E_{ijk} is the corresponding strain kernel.

In order to evaluate the domain integral in Eq. (1), the initial stress increments $\dot{\sigma}^p_{jk}$ at interior points must be determined. First, we determine the stress increments at interior points using the following

*Correspondence addressee

integral equation.

$$\dot{\sigma}_{ij} = \int_{\Gamma} U_{ijk} \dot{t}_k d\Gamma - \int_{\Gamma} T_{ijk} \dot{u}_k d\Gamma + \int_{\Omega} E_{ijkl} \dot{\sigma}^0_{kl} d\Omega + g_{ij}(\dot{\sigma}^0_{kl}) \tag{2}$$

In the initial strain approach, the terms E_{ijk}, E_{ijkl}, $\dot{\sigma}^0_{kl}$ and the free term $g_{ij}(\dot{\sigma}^0_{kl})$ should be replaced with Σ_{ijk}, Σ_{ijkl}, $\dot{\varepsilon}^0_{kl}$ and $f_{ij}(\dot{\varepsilon}^0_{kl})$, respectively, (Telles, 1983; Banerjee and Davies, 1984).

The integrals in Eqs. (1) and (2) are interpreted in the Cauchy principal value sense. In the numerical implementation, to evaluate these integrals, the boundary Γ is discretized into boundary elements and the domain Ω (or, more usually, the expected yield region) into interior cells. Displacements, tractions and stresses are expressed in terms of their nodal values. When the source point is close to the field point, the integration kernels exhibit the following singularities (Telles, 1983; Banerjee, 1994)

$$\begin{cases} U_{ij} \to O(\ln r), & U_{ijk} \to O(1/r) \\ T_{ij} \to O(1/r), & T_{ijk} \to O(1/r^2) \\ E_{ijk} \to O(1/r), & E_{ijkl} \to O(1/r^2) \end{cases} \tag{3}$$

for 2D problems, and

$$\begin{cases} U_{ij} \to O(1/r), & U_{ijk} \to O(1/r^2) \\ T_{ij} \to O(1/r^2), & T_{ijk} \to O(1/r^3) \\ E_{ijk} \to O(1/r^2), & E_{ijkl} \to O(1/r^3) \end{cases} \tag{4}$$

for 3D problems. In expressions (3) and (4), r is the distance between the source point and field point.

When the source point coincides with the field point, strongly singular integrals (both from the boundary integrals and domain integrals) arise, so special integration schemes are necessary. To evaluate the strongly singular boundary integrals, a number of techniques are available (Cruse and Richardson, 1996; Guiggiani and Gigante, 1990). Methods for the efficient evaluation of the strongly singular domain integrals in Eqs. (1) and (2) can be found in references (Mustoe, 1984; Dallner and Kuhn, 1993; Gao and Davies, 1998) and (Gao and Davies, 1999).

When the source point is not located in the integration cell, standard Gaussian quadrature can be used to evaluate all the integrals in Eqs. (1) and (2), since r is non-zero. However, when the sizes of adjacent cells are significantly different, the integrals in Eqs. (1) and (2) become nearly singular. For example, Fig. 1 shows a typical application where cells of different sizes might arise. (In this example, a rectangular plate is subjected to uniaxial tension, under plane stress conditions.)

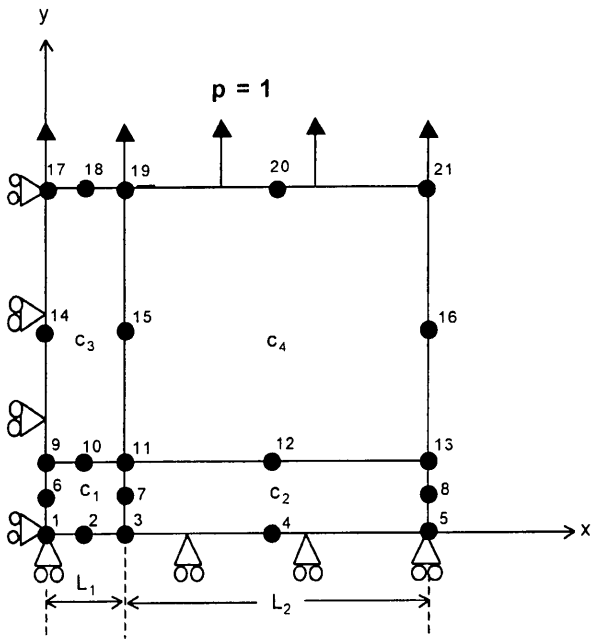

Fig. 1 BEM mesh for a 2D square plate under uniaxial tension

In Fig. 1, the sizes of the internal cells c_1 to c_4 differ substantially in size. Thus, for example, node 7 is relatively near to cell c_4 and, also, the boundary element defined by nodes 3, 4 and 5. Hence, for node 7, the integrals over c_4 and the boundary element (345) are nearly singular. Consequently, computation of these integrals is difficult. To obtain acceptable results for such integrals, many Gauss quadrature points are required. Cell (or element) subdivision is a convenient means to distribute the Gauss points in the most efficient manner.

III. SUB-DIVISION TECHNIQUE FOR NEARLY SINGULAR INTEGRALS

The Gauss quadrature formula (with abcissae x_k and weights w_k) (Stroud and Secrest, 1966) is:

$$\int_a^b f(x)dx = L \sum_{k=1}^{n} w_k f(x_k) + E_n \tag{5}$$

with the error:

$$E_n = \frac{L^{2n+1}(n!)^4}{(2n+1)[(2n)!]^3} f^{(2n)}(\xi), \quad a \le \xi \le b \tag{6}$$

in which, n is the order of the Gauss integration, and:

$$L = b - a \tag{7}$$

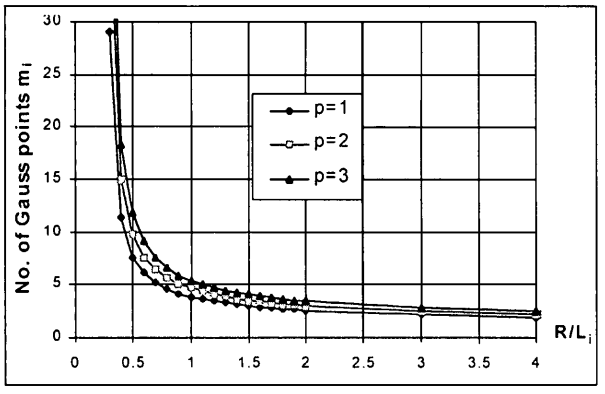

Fig. 2 Gauss integration order (after Mustoe [1])

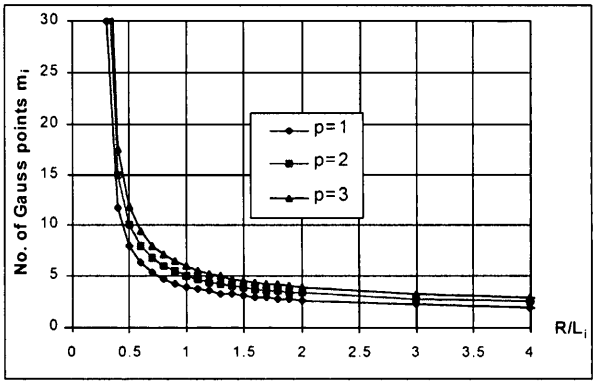

Fig. 3 Gauss integration order (from equation (10))

In the boundary element context, the parameter L can be interpreted as the length of the boundary element (or cell) along the integration direction. Thus, from equation (6) we can see that the error of the Gauss quadrature depends on the number of Gauss points and the element size. To achieve consistent accuracy for all elements through the body, larger elements must be divided into sub-elements. We now consider two criteria which have been employed to determine the Gauss integration order.

1. Lachat and Watson's Criterion

Lachat and Watson (1976) implemented algorithms to automatically select the order of integration over two or three dimensional boundary elements based upon Gaussian quadrature error bounds. An extension and generalisation of this approach was presented by Mustoe (1984).

The N-dimensional Gaussian quadrature formula can be expressed in the intrinsic co-ordinate system by:

$$V_I = \int_{-1}^{1} \cdots \int_{-1}^{1} f(\xi_1, \xi_2, \cdots, \xi_N) d\xi_1 d\xi_2, \cdots, d\xi_N$$

$$= \sum_{i=1}^{m_1} \sum_{j=1}^{m_2} \cdots \sum_{\alpha=1}^{m_N} w_i^1 w_j^2 \cdots w_\alpha^N f(\xi_1^i, \xi_2^i, \cdots \xi_N^\alpha) + E \qquad (8)$$

where ξ_1^i, ξ_2^j, ..., ξ_N^α are the Gauss points, $w_i^1 w_j^2$, ..., w_α^N are the weighting factors, m_i is the number of Gauss points in the i-th direction and E is the total integration error, i.e., $E=\sum_{i=1}^{N} E_i$ with E_i being the integration error in i-th direction. Approximate formulas for an upper bound of the relative error E_i/V_I are given by Mustoe (1984):

$$\frac{E_i}{V_I} < 2\left(\frac{L_i}{4R}\right)^{2m_i} \frac{(2m_i + p - 1)!}{(2m_i)!(p-1)!} < e_i \qquad (9)$$

where p is the order of singularity of the integrand ($1/r^n$), e_i is the prescribed tolerance of the relative integration error, L_i is the length of the boundary element in the i-th direction, and R is the minimum distance from the field point to the boundary element. Fig. 2 shows the relationship between Gauss order and the ratio of R/L_i for $e_i=5\times10^{-5}$.

From Eq. (9) we can see that if R/L_i is small, then the required Gauss order is large. For a prescribed upper limit on Gauss order, elements must be subdivided into sub-elements using (9). However, for a given value of m_i, one can only calculate the ratio of R/L_i, from Eq. (9), by iteration (Mustoe, 1984). For efficiency, in this paper, we suggest the approximation:

$$m_i = \frac{p' \ln(e_i/2)}{2\ln[L_i/(4R)]} \qquad (10)$$

which yields:

$$L_i = 4R\left(\frac{e_i}{2}\right)^{\frac{p'}{2m_i}} \qquad (11)$$

where

$$p' = \sqrt{\frac{2}{3}p + \frac{2}{5}} \qquad (12)$$

Fig. 3 shows the resulting approximate relationship between m_i and R/L_i, for $e_i=5\times10^{-5}$.

Comparing Fig. 2 with Fig. 3, it is clear that Eq. (10) is an excellent approximation to Eq. (9). It should be noted that R/L_i may not be less than 0.25, since then the integration order grows to infinity. This restriction is similar to that employed by Dallner and Kuhn (1993). The advantage of Eq. (10) is that we can directly calculate the Gauss order mi, rather than through iteration. Or, given a maximum Gauss order, Eq. (11) yields the sizes of the sub-elements directly.

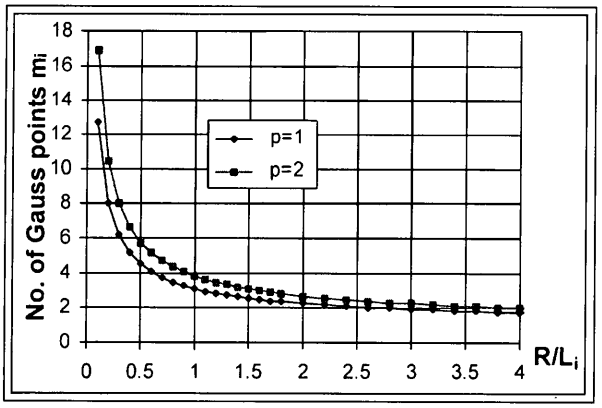

Fig. 4 Gauss integration order (after Davies and Bu [3])

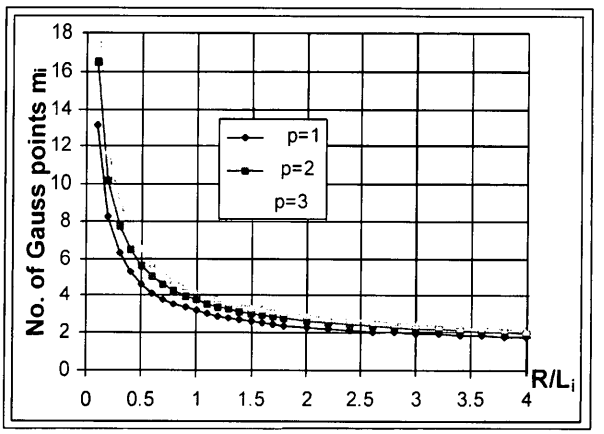

Fig. 5 Gauss integration order (from equation (15)

2. Davies and Bu's Criteria

Davies and Bu (1995) suggested a criterion based on numerical tests for surface integrals, which can be expressed (for $e_i=10^{-4}$) as:

$$m_i=\left(\frac{8L_i}{3R}\right)^{\frac{3}{4}}+1 \tag{13}$$

for integrand of $O(1/r)$, and,

$$m_i=\left(\frac{4L_i}{3R}\right)^{\frac{3}{4}}+1 \tag{14}$$

for integrand of $O(1/r^2)$. These equations are plotted in Fig. 4.

In order to take into account integrands of $O(1/r^3)$, the following unified criterion is proposed here for the three cases (p=1, 2 and 3) with the error tolerance e_i, namely:

$$m_i=p'[-\ln(e_i/2)/10]\left[\left(\frac{8L_i}{3R}\right)^{\frac{3}{4}}+1\right] \tag{15}$$

where p' is determined from Eq. (12). This equation is plotted in Fig. 5 for $e_i=10^{-4}$.

Again, comparing Figs. 4 and 5, we observe that Eq. (15) provides a very good approximation for Eqs. (13) and (14). From (15), we can calculate the maximum length L_i of a sub- element as follows:

$$L_i=\frac{3}{8}R\left(\frac{-10m_i}{p'\ln(e_i/2)}-1\right)^{\frac{4}{3}} \tag{16}$$

3. Calculation of Sub-Element Length L_i

In any element, Cartesian co-ordinates can be determined from the nodal values, i.e.,

$$x_j=\sum_{\alpha=1}^{N_e}N_\alpha(\xi_i)x_j^\alpha \tag{17}$$

where $N_\alpha(\xi_i)$ with i=1, ..., N (N is the number of intrinsic coordinates), are the shape functions (Gao, 1999), N_e is the number of the nodes defined over the element, and x_j^α is the coordinate value at node α in the j-th direction.

In this paper, the length of a boundary element is characterised by the length of the curve through the centre of the element along the integration direction, which can be accurately calculated using:

$$L_i=\int_{-1}^{1}\sqrt{\sum_{j=1}^{N_d}\left(\frac{\partial x_j}{\partial\xi_i}\right)^2}\,d\xi_i=\int_{-1}^{1}\sqrt{\sum_{j=1}^{N_d}\left(\sum_{\alpha=1}^{N_e}\frac{\partial\tilde{N}_\alpha}{\partial\xi_i}x_j^\alpha\right)^2}\,d\xi_i \tag{18}$$

where N_d=2 for 2D problems and N_d=3 for 3D problems. $\tilde{N}_\alpha$ is simply the degenerate form of the shape function $N_\alpha(\xi_i)$, in which all intrinsic co-ordinates are set to zero but the i-th one, i.e., $\tilde{N}_\alpha=N_\alpha(0, ..., \xi_i, ..., 0)$.

4. Calculation of Minimum Distance R

There is no direct method of calculating the minimum distance (R) from the source point x_j^s to an element. In this paper, the Newton-Raphson iterative scheme is employed to calculate the intrinsic co-ordinates (ξ_i) on the element boundary closest to the source point (the proximal point). We let r_j be the error in the computation of the j-th component of the global coordinates of the source. Now, the notation r_j^k, ξ_i^k is used to denote the values after the k-th iteration, i.e.,

$$r_j^k=\sum_{\alpha=1}^{N_e}N_\alpha(\xi_i^k)x_j^\alpha-x_j^s \tag{19}$$

To obtain improved values of ξ_i, we expand (19) using Taylor's theorem:

$$r_j^{k+1} = r_j^k + \frac{\partial r_j}{\partial \xi_i}\Delta\xi_i = r_j^k + \sum_{\alpha=1}^{N_e} \frac{\partial N_\alpha}{\partial \xi_i} x_j^\alpha \Delta\xi_i \qquad (20)$$

where $\Delta\xi_i$ are the changes in ξ_i. Setting r_j^{k+1} equal to zero, we obtain (in matrix form):

$$[K^k]\{\Delta\xi\} = -\{r^k\} \qquad (21)$$

where

$$[K^k]_{ji} = \sum_{\alpha=1}^{N_e} \frac{\partial N_\alpha}{\partial \xi_i} x_j^\alpha \Delta\xi_i \qquad (22)$$

Solving Eq. (21) for $\{\Delta\xi\}$, the updated values of ξ_i are:

$$\xi_i^{k+1} = \xi_i^k + \Delta\xi_i \qquad (23)$$

The proximal point on the element is determined from the equations:

$$\xi_i = \xi_i^{k+1} \qquad (\text{if } -1 \le \xi_i^{k+1} \le 1)$$

$$\xi_i = \mathrm{Sgn}(\xi_i^{k+1}) \quad (\text{if } \xi_i^{k+1} > 1 \text{ or } \xi_i^{k+1} < -1) \qquad (24)$$

The minimum distance can then be calculated from the equation:

$$R = \sqrt{\sum_{j=1}^{N} R_j^2} \qquad (25)$$

where, R_j is the j-th component of the minimum distance and is determined from the intrinsic coordinates of the proximal point:

$$R_j = \sum_{\alpha=1}^{N_e} N_\alpha(\xi_i) x_j^\alpha - x_j^s \qquad (26)$$

These calculations (Eqs. 19-26) are iterated until satisfactory convergence (of R) is attained. However, for highly distorted elements (that is, elements where the intrinsic coordinate axes are appreciably curved) convergence may be difficult to achieve. In these cases, extensive trials have demonstrated that satisfactory results (within a few percent) can be obtained by simply taking the first (local) minimum value of R.

For domain integrals over a cell, Eq. (21) can be used directly. However, for boundary integrals, the number of equations is (one) greater than the number of unknowns. In this case, Eq. (21) should be replaced by the least-squares approximation:

$$[K^k]^T[K^k]\{\Delta\xi\} = -[K^k]^T\{r^k\} \qquad (27)$$

where the superscript T implies the matrix transpose.

Excellent convergence is achieved using this iterative scheme. In general, three iterations are sufficient for an accuracy of $|\Delta\xi_i| < 10^{-6}$.

5. Adaptive Integration Scheme

The adaptive integration scheme employs an element sub-division technique. This can be done in various ways (Mustoe, 1984; Lachat and Watson, 1976; Dallner and Kuhn, 1993). The strategy which we adopt is as follows:

(a) Calculate element length L_i and minimum distance R to source using Eqs. (18)-(26).
(b) Calculate the Gauss order mi using Eq. (10), or (15).
(c) If $m_i \le m_{\max}$ ($m_{\max}$ being the permitted maximal Gauss order), then apply Gauss quadrature formulae to evaluate the integral.
(d) If $m_i > m_{\max}$, calculate the permitted maximum length $L_i^{\max}$ from Eq. (11), or (16).
(e) Divide the element into N_s ($=L_i/L_i^{\max}$) equal sub-elements. Calculate the length of each sub-element L_i^s ($=L_i/N_s$). Set $n=1$.
(f) Calculate the minimum distance R_n from the source point to the n-th sub-element using equations (18)-(26).
(g) Calculate the Gauss order m_i^n for the n-th sub-element (using L_i^s and R_n) from Eq. (10), or (15).
(h) Apply Gauss quadrature formulae to evaluate the integral over the sub-element.
(i) Repeat (f)-(h) for all sub-elements.

IV. NUMERICAL EXAMPLES

A computer program ***(NLBEAS)*** has been developed for 2D and 3D non-linear boundary element analysis employing the methods described in this paper. Linear and quadratic shape functions can be used for both boundary elements and internal cells. An incremental variable stiffness iterative solution scheme is employed in the program with yield functions coded for Tresca, Von Mises, Mohr-Coulomb, and Drucker-Prager materials (Gao and Davies, 1999). In the following, two numerical examples are given. More complicated examples can be found in Gao (1999). The computation was carried out on a Pentium PC (233MHz, 64Mb RAM). Five increments and $e_i = 10^{-5}$ are used for the two examples. The maximal Gauss order is ten.

Example 1: 2D Square Plate Under Tension

The plate shown in Fig. 1 was analysed under plane-stress conditions employing the Von Mises yield criterion, with Young's modulus $E=1$, Poisson's ratio $v=0.3$, initial yield stress $\sigma_y=0.8$ and hardening

Table 1 Selected results for a square plate loaded beyond first yield

L_1/L_2		0.125	0.167	0.2	0.25	0.333	0.5	0.75	1.
u_y (1-cell)		24.44	33.19	30.12	29.30	29.99	30.00	30.00	30.00
u_y	Eq(10)	31.76	30.65	30.30	29.47	30.08	30.04	30.01	30.06
(n-cell)	Eq(15)	31.80	30.66	30.30	29.41	30.03	30.00	29.91	29.83
n	Eq(10)	81	49	36	25	16	9	4	4
	Eq(15)	25	16	9	9	4	4	1	1
E^{σ}_{2222}	1-cell	7.0573	6.4307	6.0320	5.4744	4.6457	3.3652	2.0754	1.2546
	Eq(10)	7.1199	6.5056	6.0642	5.4765	4.6435	3.3653	2.0754	1.2546
($\times 10^{-2}$)	Eq(15)	7.1197	6.5054	6.0639	5.4764	4.6433	3.3652	2.0755	1.2547

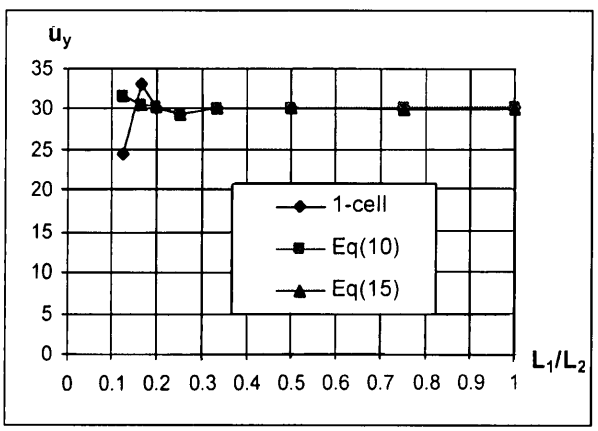

Fig. 6 Vertical displacement of plate top

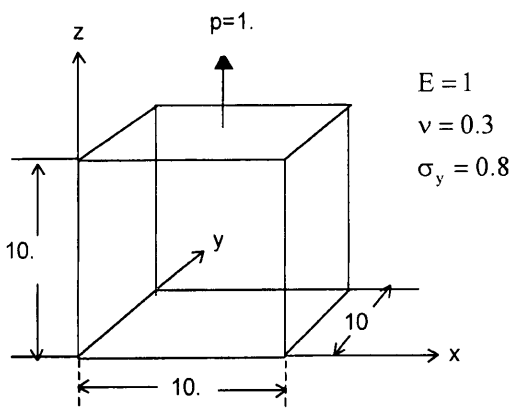

Fig. 7 A cube under tension

parameter H'=0.1. The dimension of the plate is ten. Computations were carried out for various values of L_1/L_2 and Table 1 shows some of results obtained using various strategies. In particular, data are given for the domain integral of $O(r^{-2})$ over cell 4, when the source is located at node 7.

In Table 1, the values of vertical displacement values u_y (1-cell) were obtained without using a sub-division technique and ten Gauss points were used for all integrals. The rows identified by the notation Eq. (10) and Eq. (15) denote the use of Eqs. (10) and (15), respectively. The analytical solution is u_y=30 with first yield at u_y=10. E^{σ}_{2222} is the domain integral in Eq. (2), i.e., $E^{\sigma}_{2222} = \int_{c_4} E_{2222} N_1 d\Omega$ where N_1 is the shape function of the first node of cell 4, corresponding to global node 11 in Fig. 1.

For greater clarity, Fig. 6 shows how the computed displacement u_y at the plate top is affected by the choice of discretisation scheme and integration strategy.

We observe that if the ratio of the lengths of the adjacent cells is between 0.3 and 1, all three integration schemes can give satisfactory results. However, if the ratio is smaller than 0.3, the cell sub-division technique is necessary. In general, criterion (10) gives more stable results than criterion (15), but it requires more sub-cells.

Example 2: 3D Cube Under Tension

This example is intended to examine the performance of the three integration schemes for integrands of $O(r^{-3})$ appearing in the domain integral in Eq. (2). The computational model is a cube subjected to tensile load (Fig. 7): i.e., the 3D counterpart of the plate example described above.

The cube was discretized by four boundary elements per surface and eight volume cells and the ''roller'' condition was imposed on the three planes x=0, y=0 and z=0. The meshes over the sections normal to the three planes are as shown in Fig. 1. Table 2 shows results for the displacement for the upper surface of the cube which are analogous to those obtained previously for the plate.

Again, for clarity, the displacements are plotted (in Fig. 8) in order to illustrate the differences between the results computed by using the three methods.

Similar conclusions to those drawn from the 2D case can be reached from an examination of these data. Integration without the aid of cell division

Table 2 Selected results for a cube loaded beyond first yield

L_1/L_2		0.125	0.167	0.2	0.25	0.333	0.5	0.75	1.
u_{y^*} (1-cell)		4.71	17.86	24.06	29.08	30.10	30.00	30.00	30.00
u_y	Eq(10)	33.17	30.98	30.40	30.09	30.01	30.00	30.00	30.02
(n-cell)	Eq(15)	33.08	30.98	30.59	30.08	30.02	29.97	29.99	29.98
n	Eq(10)	1331	512	343	216	64	27	8	8
	Eq(15)	125	64	27	27	8	1	1	1

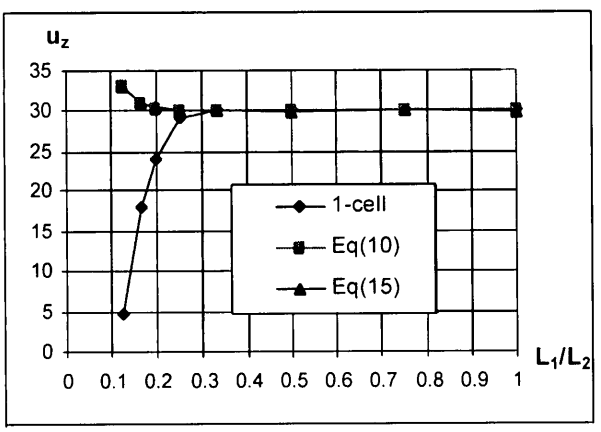

Fig. 8 Vertical displacement of cube upper surface

breaks down when cell size ratios fall below (about) 0.3. The two sub-cell criteria yield very similar results, but the second has the advantage that fewer sub-cells are needed, with a consequent saving in computational time.

CONCLUSION

An efficient adaptive integration scheme, based on cell sub-division techniques has been described, which can deal with the near singular integrals which arise in non-linear boundary element methods. In real engineering applications, robust accurate schemes such as this are essential in order to contain computational costs.

REFERENCES

1. Mustoe, G.G.W., 1984, "Advanced integration schemes over boundary elements and volume cells for two- and three-dimensional non-linear analysis," in: *Developments in Boundary Element Methods*, Elsevier, London.
2. Lachat, J.C., and Watson, J.O., 1976, "Effective numerical treatment of boundary integral equation," *Int. J. Num. Meth. Engng*, Vol. 10, pp. 991-1005.
3. Davies, T.G., and Bu, S., 1995, "Effective evaluation of non-singular integrals in 3D BEM," *Advances in Engng. Software*, Vol. 23, pp. 121-128.
4. Dallner, R., and Kuhn, G., 1993, "Efficient evaluation of volume integrals in boundary element method," *Comp. Methods in Appl. Mech. and Engng.*, Vol. 109, pp. 95-109.
5. Gao, X.W., and Davies, T.G., 1998, "Accurate evaluations of strongly singular domain integrals in non-linear BEM," In: *Boundary Elements XX* (C.A.Brebbia et al. Eds.), pp. 85-94, Computational Mechanics Publication, Southampton.
6. Telles, J.C.F., 1983, "The boundary element method applied to inelastic problems." Springer-Verlag, Berlin.
7. Banerjee, P.K., and Davies, T.G., 1984, "Advanced implementation of the boundary element methods for three-dimensional problems of elasto-plasticity." in: *Developments in Boundary Element Methods*, Elsevier, London.
8. Cruse, T.A., and Richardson, J.D., 1996, "Non-singular Somigliana stress identities in elasticity." *Int. J. Num. Meth. Engng.*, Vol. 39, pp. 3273-3304.
9. Guiggiani, M., and Gigante, A., 1990, A general algorithm for multidimensional Cauchy principal value integrals in the boundary element method. *J. Appl. Mech.*, Vol. 57, pp. 906-915.
10. Gao, X.W., and Davies, T.G., 1999, An effective boundary element algorithm for 2D and 3D elastoplastic problems." *Int. J. Solids and Structures*, (In press).
11. Stroud, A.H., and Secrest, D., 1966, Gaussian quadrature formulas. Prentice-Hall, Inc., Englewood Cliffs, NJ.
12. Banerjee, P.K., 1994, The Boundary Element Methods in Engineering. McGraw Hill.
13. Gao, X.W., 1999, "3D Non-linear and multi-region boundary element stress analysis." PhD Thesis, Glasgow University, UK, 1999.

Discussions of this paper may appear in the discussion section of a future issue. All discussions should be submitted to the Editor-in-Chief.

Manuscript Received: Nov. 15, 1999
Revision Received: Jan. 20, 2000
and Accepted: Feb. 01, 2000

彈塑性邊界元素分析之自適性積分

Xiao-Wei Gao and Trevor G. Davies
Department of Civil Engineering
Glasgow University
Glasgow G12 8LT, UK

摘 要

本文針對內部網格積分和邊界元素積分提出一個高效率的自適性積分技術。這自適性的演算法對於即使內部網格和邊界網格大小有差異時，均可一併考慮。本文採用一些數值的算例驗證本法的可行性。

關鍵詞：自適性積分，彈塑性，邊界元素法。